

A Diffusive Model for Nanoparticle Penetration into Living Cells

L. Martin, S. Collin, E. Jeandupeux, A. Deutsch, and A. Zeitoun, *Member, CBEES*

Abstract—Like any other living species, Human kind has been exposed to nanoparticles during its entire existence. But the question of their toxicity has only been raised recently as a consequence of rapid growth of industrial activity. Nowadays, the impact of nanoparticles is not clearly known. For this reason Mathematics in Medicine Study Groups (M.M.S.G.) developed a mathematical model based on the different possible entries of nanoparticles into cells. To allow further studies on their toxicity, M.M.S.G. model has been completed here by introducing adapted equations of diffusion to represent its effects on nanoparticles penetration and accumulation inside cells. It is mainly shown that due to their size (100nm), nanoparticles diffusion time is extremely short compared to characteristic system evolution time. As a consequence, living cells are not shielded against high nanoparticle bursts which enter almost instantaneously inside and equalize over all cell domain. More favourable situation could only be expected with much larger nanoparticle size.

Index Terms—Diffusion, mathematical model, nanoparticles, penetration.

I. INTRODUCTION

Though nanoparticles (NP) have always existed in their natural forms, they are today mostly the direct result of industrial activity, and their number has been following the rise of this sector during past century. Even though nanotechnologies are more and more studied in fields such as healthcare, their real impact is still difficult to evaluate in terms of nuisance and toxicity [1]-[3] as it depends on both penetration inside cells and local specific action. Unlike usual particles, NP toxicity, aside its mass, also depends on many other parameters such as charge, size, shape, composition, porosity and surface structure. Specific surface (i.e. the ratio surface/mass), is particularly important as it determines thresholds for many interactions with other organisms. NPs can also be vehicle for pollutants in suspension in the atmosphere, as they can absorb on their surface toxic molecules for the organism once inhaled or brought in by any means. This induced toxicity is still difficult to estimate and to model. For completeness, NP can be acting on different cells through rejected vesicles. NP has been defined as nano-object whose all three dimensions are less than 100 nm. At this very small size, the physical properties of a material change and the possibility of penetration inside human body is higher [3], [4]. So it is necessary to set down a faithful representative mathematical model for correctly describing their internalisation into a cell in order to find later clues about their toxicity [1], [5]-[7]. It

is the intention to report here a step toward such a model developed through easy-to-work and open MATLAB software, in order to analyze physical effects at the origin of cell penetration by NPs. The work is based on a model proposed by the Mathematics in Medicine Study Group (M.M.S.G.) [4].

This is mainly a homogeneous compartment model neglecting the detailed influence of diffusion on NP flux into cells. However averaged values are not sufficient for precise determination of toxicity thresholds which are also related to maximum values for direct action. So diffusion effects have to be taken care of, and extension of 0 D M.M.S.G. model to 1D and 2D ones is discussed in present paper. Effects of inward speed on diffusion and maximum flux values are discussed and enhancement of NPs penetration is evaluated. The effect of NP size on their diffusion into the cell is also analyzed as this is an important parameter for diffusion coefficient.

II. M.M.S.G. MODEL

M.M.S.G. model is a 0D compartment model describing the three main penetration ways of NP into cell

- endocytosis (by a fluid and a receptor)
- diffusion or disruption
- passage by ionic channel

by decreasing order of importance. There are three compartments: the boundary area B surrounding cell membrane, the cell membrane M and the cell volume I , see Fig. 1 M.M.S.G. 0D model is thus a set (S) of five 2nd degree nonlinear ordinary differential equations with five time dependent unknowns B , M , I , L and H .

$$\begin{aligned} dB/dt = & -k_1 B(M^{max} - M) + k_2 M + k_3(B_{ss} - B) \\ & - k_{4f} BL + k_5(I - B) - k_6 H(B - I) \end{aligned} \quad (1)$$

$$dM/dt = k_1 B(M^{max} - M) - k_2 M - k_{4r} ML \quad (2)$$

$$\begin{aligned} dI/dt = & k_{4r} ML + k_{4f} BL - k_5(I - B) \\ & + k_6 H(B - I) \end{aligned} \quad (3)$$

$$dH/dt = k_7 B + k_8 I - k_9 H \quad (4)$$

$$dL/dt = k_{10}(L_{inf} - L) - k_{4r} LM - k_{4f} BL \quad (5)$$

The first three variables B , M , I represent average NP distributions in each of the three compartments. L is the size of lipids in the membrane and H is the number of holes created by specific internalization. The fluctuations are functions of the different ways of penetration and the various “ k_x ” factors represent the likelihood of an exchange

as compared to another one. Adding (1),(2),(3) one gets

$$d(B+M+I)/dt = k_3(B_{ss}-B) \quad (6)$$

so $B+M+I = C_0$ a constant when $k_3 = 0$ allowing to reduce (S) to four equations. Letting $l=L/B_{ss}$, $m=M/B_{ss}$, $i=I/B_{ss}$, $h=H/B_{ss}$, $b=B/B_{ss}$, stationary solution of (1),(2),(3), (4),(5) can be found in the form $b=1$ from (6) and

$$l=l_{inf}-(k_5B_{ss}/k_{10})i; h=(k_7+k_8)/k_9+(k_8/k_9)i \quad (7)$$

$$m=m_0-m_1i+m_2i^2 \quad (8)$$

where $m_2=(k_6k_8/k_9)B_{ss}$ and m_0, m_1 are expressed in terms of the various k_j , and i is solution of 3rd order equation

$$\Delta(i) \equiv k_{4r}ml + k_{4r}l - k_5B_{ss}i = 0 \quad (9)$$

such that $\Delta(0) > 0$ and $\Delta(i) \rightarrow -\infty$ when $i \rightarrow \infty$. This implies that there exists a positive solution i_{stat} to which $i(t)$ converges, and so are doing the other components. From expressions of the various coefficients, it is not possible to reduce (S) on the only base of smallness of some k_j . It should first be ascertain that there corresponds a nontrivial solution to such a reduction. For instance calling (S₀) the model where one sets $k_3 = k_{4r} = k_5 = k_6 = k_7 = k_8 = k_9 = 0$ owing to the smallness of these parameters, which eliminates (4) for H , this would lead to stationary solution

$$M=B=0, L=L_{inf}, I=I_0 \quad (10)$$

which may not be always appropriate everywhere as mentioned below.

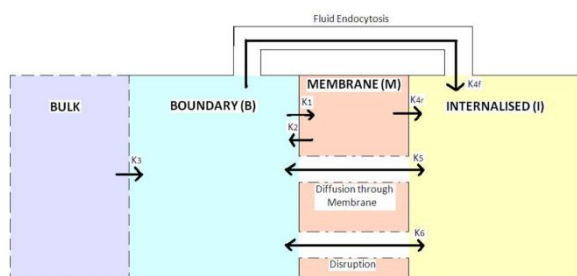


Fig. 1. Schematic display of system compartments from M.M.S.G. It represents interactions between the different compartments of a cell.

Boundary, Membrane and Internalized are compartments used in M.M.S.G model and Bulk is outside the cell where Np cannot interact with the cell. The large arrows represent the three of four main penetration ways explained at the beginning of part II. “kx” factors are ratio which represent the likelihood of an exchange as compared to another one and used in the MMSG 0D model. k1: Binding of NP to membrane; k2: Unbinding of NP from membrane; k3: Replenishment of NP; k4r: Receptor mediated endocytosis; k4f: Fluid-phase endocytosis; k5 Diffusion through membrane; and k6: Disruption mediated diffusion

To numerically solve the problem, MATLAB software has been preferred to multi-physics non-linear PDE solver FreeFEM++ mainly competitive for more general geometrical domains. 4th order Runge-Kutta method appears as more adapted to present problem than Euler one because of better conservation of system properties.

III. DIFFUSION MODEL

Diffusion is a very general phenomenon occurring in gaseous, liquid and solid environments. It concerns the different ways of specific particles which are behaving under possible outer action in the presence of all the other particles in the medium. Experiments have shown that their displacement is a Brownian, i.e. random, motion. Addition of diffusion effect in M.M.S.G. model is intended to account for its role on inhomogeneity of final internal NP distribution. This will lead to better evaluation of this distribution, and in particular to define its maximum inside the cell, an important element in toxicity measurement. In addition, the role of diffusion will be determined on every component of state functions B, M, I, L and H in the model.

Rewriting system (1), (2), (3), (4), (5) in compact form

$$dX/dt = A \cdot X + B : XX = F(X) \quad (11)$$

where $X = \text{col}[B, M, I, H, L]$ and A and B stand for the k_x coefficients of linear and nonlinear terms respectively. Diffusion model constructed from (11) takes then the form:

$$\partial_t U - \alpha \Delta U = A \cdot U + B : UU = F(U) \quad (12)$$

where Δ is Laplacian operator ($= \partial_x^2$ and $\partial_x^2 + \partial_y^2$, respectively for 1D and 2D systems). $U = U(x, t) = \text{col}\{B(x, t), M(x, t), I(x, t), H(x, t), L(x, t)\}$ is a 5-space time dependent vector, $x=x_1$ for 1D and $x=(x_1, x_2)$ for 2D. $\alpha = \text{diag}[\alpha_b, \alpha_m, \alpha_i, \alpha_h, \alpha_l]$ represents the diagonal matrix of diffusion coefficients for each component studied in the model. To figure out diffusion effect with respect to homogeneous 0D M.M.S.G. model, the two quantities $U_{max}(t) = \text{Max}_x U(x, t)$ and $\langle U(x, t) \rangle = \int dx U(x, t)$ will be examined. It can be observed from (11) and (12) that at equilibrium there exists the relation

$$F(\langle U_{eq} \rangle) = -\alpha n \cdot \nabla U|_S - \mathcal{B} : \langle \delta U \delta U \rangle \quad (13)$$

Writing $U = \langle U \rangle + \delta U$ with $U_{eq}(x)$ the asymptotic limit of $U(x, t)$ when $t \rightarrow \infty$, and $n \cdot U|_S$ is the boundary condition at limit surface S . So $\langle U_{eq} \rangle \neq \lim_{t \rightarrow \infty} X(t)$ unless the two terms on the right hand side are 0. Such result extends easily to any nonlinear interaction function $F(U)$ with more complicated $\langle \delta F / \delta U \rangle$ instead of $\mathcal{B} \langle \delta U \delta U \rangle$.

For resolution the Splitting method has been used. It enables to solve two problems by first treating each problem and to superimpose the two intermediate results to get the final one.

Entrance of NPs in the cell varies depending on their characteristics such as size [8]-[10] because diffusion inside the cell is inversely proportional to NP radius [11]. The diffusion coefficient is given by Stokes-Einstein equation: $D = kT / (6\pi\eta r)$ with k the Boltzmann constant, T the temperature in K, η the viscosity in $\text{kg} \cdot \text{m}^{-1} \cdot \text{s}^{-1}$, r the radius of the particle in meters which influences results for M, B, L and I . Curves for diffusion coefficient vs size of NP are displayed on Fig. 2. Consequently, it is much faster to calculate any function by inputting NP radius instead of entering all diffusion coefficients each time in the equations.

Flux calculations have been performed with both diffusive 1D and 2D system (12) respectively, and with

simplified versions of (S). It is verified that same results are mainly obtained in the two cases.

Three different boundary conditions are used:

- Dirichlet boundary conditions by imposing a fixed value on the edges
- Neumann boundary conditions on derivative values
By imposing a constant flow
By blocking entrance and exit on the edges

The value of each diffusion coefficient from each compartment has been evaluated. According to the areas for B , M , I , H and L , diffusion coefficients are 10^{-7} , 10^{-8} , 3.310^{-6} , 0 , 6.110^{-7} , respectively (cm²/s).

These values have been adapted to fit the proportions in the simulation, and have been multiplied by 10^5 . In a general way, diffusion coefficient scales as $\alpha \approx (\Delta l)^2 / \Delta \tau$ where Δl $\alpha v \delta$ $\Delta \tau$ are characteristic length and time scale. As $\alpha = K / r_p (r_p$ particle dimension), from Stokes-Einstein equation one gets by equating the two expressions of α

$$\Delta \tau = K^{-1} (\Delta l)^2 \rho_{\pi} \quad (14)$$

Two consequences can be drawn from (14). If $\Delta l = l_c$ the typical cell size, $\Delta \tau = T_{diff}$, the diffusion time which is shorter as r_p is smaller, and may be extremely small compared to natural (non diffusive) system evolution time T_n , as fixed from 0D model for instance. On the other hand, if space mesh size for numerical resolution is $\Delta l = l_c / N$, N large enough integer, explicit scheme stability requires that time step be $\Delta \tau_{calc} < \Delta \tau_{stab} = K^{-1} (\lambda_{\gamma} / N)^2 r_p = T_{diff} / N^2$ which may be extremely small, and would lead to very long calculation for following system evolution up to T_n .

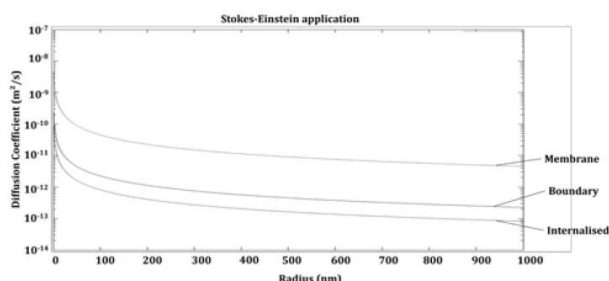


Fig. 2. Curve which represents evolution of diffusion coefficient depending on nanoparticle radius for different compartments (membrane, boundary and internalised). This curve use Stokes-Einstein application.

IV. 1D RESULTS

As expectable, diffusion influences internalisation speed and the curves of $\langle B \rangle$, $\langle M \rangle$, $\langle I \rangle$, $\langle H \rangle$ and $\langle L \rangle$ converge both for the initial rectangular and Gaussian initial conditions.

A. Initial and Boundary Conditions

Three types of initial conditions are considered: slot function, Gaussian function (and reverse function), rectangular function (and reverse function).

Slot initial conditions are defined by $B(t=0)=1$, $M(t=0)=0$, $I(t=0)=0$, $H(t=0)=0$ and $L(t=0)=1$. Initial conditions represented by a rectangular step and their reverses are defined by the “unit” scale level 0.25 indicating that NPs are supposed to be internalised only at one extremity of the cell. Initial conditions are $I(x < 0.25, t=0)=1$ and $I(x > 0.25, t=0)=0$.

Other initial conditions are $B(x < 0.25, t=0) = M(x < 0.25, t=0) = L(x < 0.25, t=0) = 0$ and $B(x > 0.25, t=0) = M(x > 0.25, t=0) = L(x > 0.25, t=0) = 1$ with $H(x, t=0)=0$. Initial conditions can also be represented by a Gaussian distribution. As with previous initial conditions, other unknown elements such as B , M and L have values opposite to case I except for H , which remains equal to zero because it is supposed that there were no previous internalisation. Thus one will set:

$$B(x, t = 0) = M(x, t = 0) = L(x, t = 0) = 1 - I(x, t = 0) \quad (15)$$

with $I(x, t=0) = \exp\{15(x-0.5)^2\}$.

B. 1D Qualitative Results

Variation of maximum $U_{max}(t)$ in each compartment has been checked with and without diffusion. Strong decrease of $\langle M \rangle$ at the beginning can be explained as a particle saturation in corresponding area leading to particle displacement toward neighbouring areas, with corresponding small increase of $\langle B \rangle$. Moreover, when initial condition is a Gaussian, the $\langle I \rangle$ curve can be explained by a very slow filling up until maximum is reached which increases I until particle stabilization inside the cell.

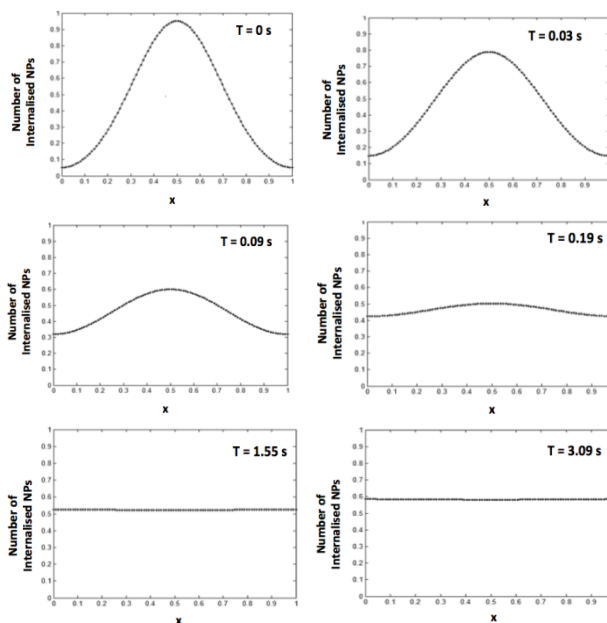


Fig. 3. 1D Profile Time Evolution for $\langle I(x, t) \rangle$ (Internalised) at different times ($T=0$ second, $T=0.03$ seconds, $T=0.09$ seconds, $T=0.19$ seconds, $T=1.55$ seconds, $T=3.09$ seconds). It represents the number of internalised nanoparticles based on x .

Addition of diffusion to the model produces fast decrease of $\langle B \rangle$ and $\langle I \rangle$, which can be explained by attenuation of the Gaussian by diffusion into the cell. After this short initial period, the two curves exhibit the same convergence as the corresponding ones without diffusion, as verified from profile evolution at early time, see Fig. 3. It can be checked that, due to actual parameters value, internal NP profile becomes completely flat after 3 time units, and 0D system is valid after this very short diffusion time.

Fig. 4 displays the graphs representing average NP distribution $\langle U \rangle(t)$ for Gaussian initial conditions. Observed convergence for all components $\langle B \rangle$, $\langle M \rangle$, $\langle I \rangle$,

$\langle H \rangle$, and $\langle L \rangle$, as expectable from stability of 0D M.M.S.G. model, is occurring after a time $T_n \gg T_{diff}$.

TABLE I: QUANTITATIVE RESULTS FOR RECTANGULAR AND GAUSSIAN INITIAL CONDITIONS

Compartment	Acceleration rectangular (%)	Acceleration Gaussian (%)
Boundary	1.82	1.84
Internalised	3.41	3.43
Holes	3.14	3.29
Membrane	1,80	1,80
Lipid	2,73	2,67

This is confirmed by evaluating convergence times for each component with and without diffusion as displayed on Fig. 5. Despite differences from (13) they are very similar for same initial conditions.

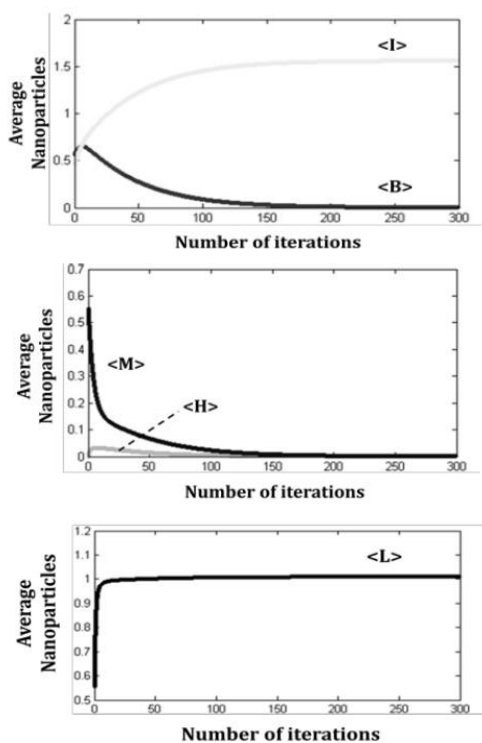


Fig. 4. Convergence of $\langle B \rangle$, $\langle M \rangle$, $\langle I \rangle$, $\langle H \rangle$ and $\langle L \rangle$ with Gaussian Initial Conditions ($\langle B \rangle$ for Boundary, $\langle M \rangle$ for Membrane, $\langle I \rangle$ for Internalised, $\langle H \rangle$ for Holes, $\langle L \rangle$ for Lipid Size). Curves represent average nanoparticles based on number of iterations.

C. 1D Quantitative Results

For finer analysis, the point of convergence has been taken at the time where the components ($\langle B \rangle$, $\langle I \rangle$, $\langle H \rangle$, $\langle M \rangle$ or $\langle L \rangle$) are reaching a given value (for example when boundary component has reached a sum of 10^{-2}). This value is considered as the final value with corresponding time value. Below are the results of acceleration internalisation speed with and without diffusion.

The results are about the same for Gaussian and rectangular initial conditions. This can be explained by the fact that rectangular condition will rapidly transform into

Gaussian one with diffusion. The time to transform the rectangle into a Gaussian can explain the fact that percentages are higher for the Gaussian.

It is observed from Fig. 3 that only $\langle L \rangle$ and $\langle I \rangle$ are taking finite values for $t \rightarrow \infty$. According to (10) this would justify simplification of (S) into (S₀) if one is interested in large time evolution only.

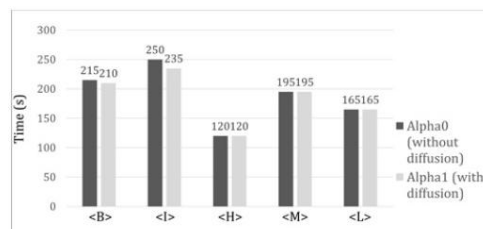


Fig. 5. A histogram showing convergence time for $\langle B \rangle$, $\langle M \rangle$, $\langle I \rangle$, $\langle H \rangle$ and $\langle L \rangle$ with (left column) and without (right column) diffusion and gaussian initial conditions ($\langle B \rangle$ for boundary, $\langle M \rangle$ for membrane, $\langle I \rangle$ for internalised, $\langle H \rangle$ for holes, $\langle L \rangle$ for lipid size).

V. 2D RESULTS

2D NP diffusion is integrated using Cartesian coordinates in order to match true cell proportions.

Results of M.M.S.G. model have been used as initial values to solve the problem for using Splitting method as for 1D model. The study is resting on a simplified square shape cell in Cartesian coordinates. Approximation is possible because the model deals with very small dimensions.

A. Initial and Boundary Conditions

Like for 1D case, a Gaussian function has been taken for I with a mean in the middle of the square for compartment I . Initial conditions for other compartments are deduced exactly in the same way as in 1D, i.e. $1-I(x, t=0)$ for B , M and L , and 0 for H . This initial condition is the one where diffusion can clearly be observed.

Neumann boundary condition has been used with blocking entrance and exit at the edges because it is the more efficient.

B. Results

As for 1D case, 2D convergence analysis is showing similar results, see Fig. 6.

The curves are again showing sharp changes at very short initial time. Analysis of full2D system evolution at these very early beginning times is better followed with adapted color scale, see Fig. 7.

As diffusion coefficients are different, diffusion speeds are different in each compartment, but in last one component I behaves differently. Here after $T=0.32$ colors are reversing, showing that in the cell domain NP accumulate in different places as shown by comparing $T=.08$ to $T=.39$ for instance. There are two reasons for this phenomenon. On the one hand, larger gradient in NP distribution has stronger effect to make it more homogeneous. On the other hand, higher NP distributions in neighboring compartments B and M are with same gradient launching more NP into I compartment. When $k_3=0$ $B+M+I$ is constant and their distributions balance each other.

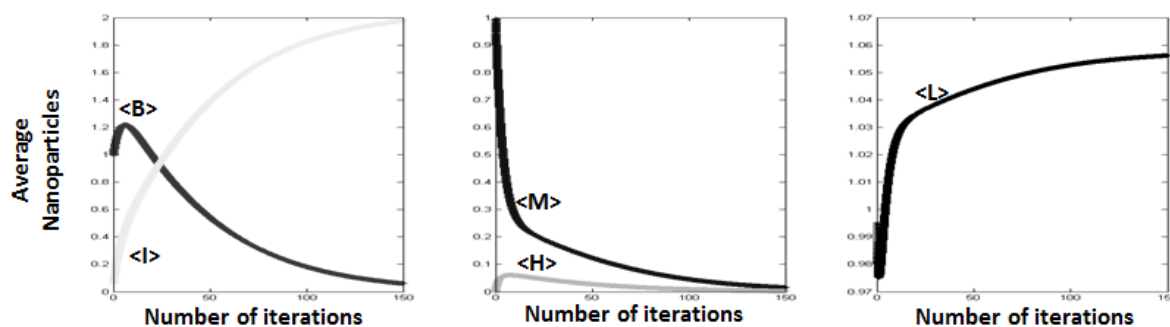


Fig. 6. Curves showing convergence of $\langle B \rangle$, $\langle M \rangle$, $\langle I \rangle$, $\langle H \rangle$, and $\langle L \rangle$ with gaussian initial conditions (B for boundary, M for membrane, I for internalised, H for holes, L for lipid size).

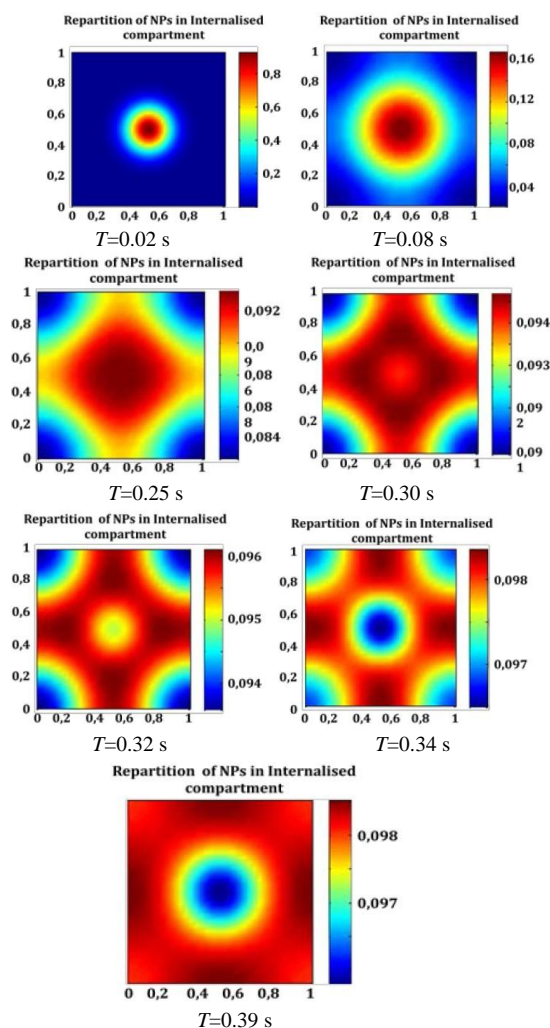


Fig. 7. Profiles showing the evolution of nanoparticles amount (representing by a color scale) in Internalised compartment called I at different times ($T=0.02$ seconds, $T=0.08$ seconds, $T=0.25$ seconds, $T=0.30$ seconds, $T=0.32$ seconds, $T=0.34$ seconds, $T=0.39$ seconds).

VI. CONCLUSION

Diffusion effect on NPs penetration into a cell has been studied in 1D and 2D space dimensions. It is mainly shown that diffusion has an important direct impact on NP penetration into the cell at early time. This is a consequence of smallness of diffusion coefficients for actual NP considered size which does not produce any shielding effect against NP entrance into the cell. So cell structure is not protected against high level impact of NPs of considered size in present paper. As present study is focused on human cells, it is thus important to take into account both the

specific nature of cell organizes (ribosome, etc.) and exocytose (as particles can get out of the cell) to have a finer balance of possible NP effect at early time.

Present model gives diffusion effect as a function of NP size, and can be completed by introducing other NP parameters such as load or shape. Also convection, which implies a material motion in local environment, can be considered for the cell in present case. This would mean to take cell motion into account at a certain speed and therefore to apply a velocity gradient to the cell.

Aside still unclear nonlinear diffusion processes, another potential improvement is to develop implicit schemes for spatial diffusive models. This implies to represent the time vector as a solution of the system and therefore to get rid of dependence on time step conditions which from (14) are the stricter as the system is a stiffer one, due to smallness of diffusion coefficients for actual value of NP dimension. This is shown by very sharp variation of $\langle L \rangle$ and $\langle M \rangle$ on Fig. 4 and Fig. 6, indicating possible and convenient system reduction by multi-time asymptotic analysis.

ACKNOWLEDGMENTS

The project has been developed within ECE Paris School of Engineering. The authors would like to particularly thank Prs. M. Belaouar and M. Hamdache for their involvement and contribution in deep mathematics knowledge, and Pr M. Cotsaftis for help in preparation of the manuscript.

REFERENCES

- [1] C. Ostiguy, G. Lapointe *et al.*, *Nanoparticles: Actual Knowledge about Occupational Health and Safety Risks and Prevention Measures*, ISBN 13: 978-2-89631-062-3, 2006.
- [2] C. Buzea, I. P. Blandino, and K. Robbie, "Nanomaterials and nanoparticles: sources and toxicity," *Biointerphases*, vol. 2, no. 4, pp. MR17-MR172, 2007.
- [3] *The French Food Safety Agency, Nanotechnologies and Nanoparticles inside Human and Animal Feed*, March, 2009.
- [4] I. Argatov, A. Davies, L. Dyson *et al.*, *How do Manufactured Nanoparticles Enter Cells?* Rept UK Mathematics-in-Medicine Study Group, Reading, 2011.
- [5] P. Smith, M. Giroud, H. Wiggins *et al.*, "Cellular entry of nanoparticles via serum sensitive clathrin-mediated endocytosis, and plasma membrane permeabilization," *Intern. J. Nanomedicine*, vol. 7, pp. 2045–2055, 2012.
- [6] H. B. Frieboes, M. Wu, J. Lowengrub *et al.*, "A Computational Model for Predicting Nanoparticle Accumulation in Tumor Vasculature," *PLoS One*, vol. 8, no. 2, p. e56876, doi:10.1371/journal.pone.0056876, 2013.
- [7] S. Kaluza, J. K. Balderhaar *et al.*, *Workplace Exposure to Nanoparticles*, European Agency for Safety and Health at Work, Literature Review.
- [8] C. L. D. Youta, *Use of Nanoparticles in Order to Provide Proteins to the Respiratory Epithelium, Characterization of Involved*

Mechanisms, University of Health and Law - Lille 2 Graduate School of Biology-Health Lille, September 3, 2012.

- [9] S. Quignard, "Silica Nanoparticles behaviour into a biological environment," Doctoral thesis, P. and M. Curie University, July 12, 2012.
- [10] O. Faklaris, D. Garrot, V. Joshi *et al.*, "Comparison of the photoluminescence properties of semiconductor quantum dots and non-blinking diamond nanoparticles," *Observation of the Diffusion of Diamond Nanoparticles in Living Cells*, 2009
- [11] M. Arroyo and A. DeSimone, *Relaxation Dynamics of Fluid Membranes*, Feb. 18, 2009.



L. Martin was born in Paris in 1992. After scholar courses, she joined an engineering school in Paris, ECE Paris. During the last two years, she chose a specialty in Health and Technology. Currently, she is a final year student and will obtain her degree in 2014.

During her studies, she has done several internships in the field of health, medicament as a summer job and medical devices as marketing

Today, she works as a marketing and clinical affairs trainee in Paris.

Ms. Martin participated in a competition as part of a previous research project and work on various publications in the context of his current work.



S. Collin was born in Clamart, France in 1992. She passed her A-Level with a specialization in Science in 2009 in the Academy of Versailles (France). Then, she spent 2 years in scientific preparatory classes for Engineering School entrance, Lycée Michelet in Vanves (92-France) (2009-2011). Finally, she joined an engineer school in Paris, ECE Paris to graduate as a generalist engineer with a specialization in health and technology. Currently, she is in master 2 and will graduate mid-2014.

Last year, she did a 4 month-internship in Advanced Research in Sorin Group (France). The challenge was to use a piezoelectric transducer to generate electrical power in a new generation of pacemaker to reduce its weight, size and power consumption and consequently make it last longer. Today, she is doing her final-year internship in the laboratory LTSI (Laboratory of Signal & Image Treatment) in collaboration with CHU

Rennes (the University Hospital Center of Rennes). The object of this 5-month internship is to study and implement a preoperative virtual planning tool for long term mechanical circulatory support. Ms Collin is planning to continue her studies to get a PhD.



of studies.

E. Jeandupeux was born in 1989 in St Aubin (Switzerland). After getting his high school diploma in 2007 he carried on studying electrical engineering and computer sciences and obtain a bachelor's degree in electronic, electrotechnic and automatic in 2011. Then he joined the ECE Paris, an engineering school where he got specialized in technologies for healthcare. He is actually working for general electric healthcare for a 6 months internship in his final year



A. Deutsch was born in Paris in December 1990. After a year in medical school, she decided to take another path and to join the engineering school ECE Paris. During the last two years, she chose a specialty in Health and Technology. Currently, she is a final year student and will obtain her degree in 2014.

During her studies, she has done several internships in the field of healthcare, such as her internship in medical research at inserm. Now, she works at the Sales Department of GE Healthcare and intends to be a product sales specialist.

works at the Sales Department of GE Healthcare and intends to be a product sales specialist.



A. Zeitoun was born in Cr èteil [the suburb of Paris] in 1990. After scholar courses, he joined an engineer school in Paris, ECE Paris. During the last two years, he chose a specialty in Health and Technology. Currently, he is a final year student and will obtain his degree in 2014.

During his studies, he has done several internships in the field of health and research as an internship in the *Institut national de la sant éet de la recherche médicale* (INSERM) to work on automatic registration in the middle ear ossicles. Today, he works at General Electric Medical System as a clinical research engineer.